From the curves in Figure 2, we can see that a cubic cavity of 40 mm side length is the most efficient in reducing the oscillator noise of an active patch antenna with intrinsically poor noise performance. However, this would increase the volume and cost of a compact active antenna. Other easy and simple approaches including using a higher ε_r substrate or using a low-noise device; even the use of a low-profile shallow cavity can also reduce the phase noise level up to 27 dB.

It was found in our experiments that, although the above noise reduction techniques can be combined together, i.e., using a low-noise device, a high ε_r substrate, and a deep cavity simultaneously, the phase noise level of the whole circuit could not be further reduced from curve 3 in Figure 2. The maximum achievable performance is ultimately decided by the device, the combined antenna Q-value, and their interaction.

ACKNOWLEDGMENT

This work was conducted under the U.K. Engineering and Physical Science Research Council (EPSRC) Contracts GR/K 75682 and GR/K 75675 as part of a joint project between Birmingham University and the Queen's University of Belfast.

REFERENCES

1. J. A. Navrro, K. A. Hummer, and K. Chang, "Active Integrated Antenna Elements," *Microwave J.*, Jan. 1991, pp. 115–126.
2. J. Birkeland and T. Itoh, "Planar FET Oscillators Using Periodic Microstrip Patch Antennas," *IEEE Trans. Microwave Theory Tech.*, Vol. 37, Aug. 1989, pp. 1232–1236.
3. C. H. Ho, F. Lu, and K. Chang, "New FET Active Slot Ring Antenna," *Electron. Lett.*, Vol. 19, Mar. 1993, pp. 521–522.
4. M. Zheng, Q. Chen, P. S. Hall, and V. F. Fusco, "Oscillator Noise Reduction in Cavity-Backed Active Microstrip Patch Antenna," *Electron. Lett.*, Vol. 33, July 1997, pp. 1276–1277.
5. J. Lin and T. Itoh, "Active Integrated Antennas," *IEEE Trans. Microwave Theory Tech.*, Vol. 42, Dec. 1994, pp. 2186–2194.
6. M. A. Gouker, J. T. Delisle, and S. M. Duffy, "A 16-Element Subarray for Hybrid-Circuit Tile-Approach Spatial Power Combing," *IEEE Trans. Microwave Theory Tech.*, Vol. 44, Nov. 1996, pp. 2093–2098.
7. I. Goldstein, "Frequency Stabilization of a Microwave Oscillator with an External Cavity," *IRE Trans. Microwave Theory Tech.*, Vol. MTT-5, Jan. 1957, pp. 57–62.

CCC 0895-2477/98

ANALYTICAL DERIVATION OF A CONFORMAL PERFECTLY MATCHED ABSORBER FOR ELECTROMAGNETIC WAVES

F. L. Teixeira[1] and W. C. Chew[1]
[1] Center for Computational Electromagnetics
Electromagnetics Laboratory
Department of Electrical and Computer Engineering
University of Illinois at Urbana – Champaign
Urbana, Illinois 61801-2991

Received 29 September 1997

ABSTRACT: *We present an analytical derivation of a 3-D conformal perfectly matched layer (PML) for mesh termination in general orthogonal curvilinear coordinates. The derivation is based on the analytic continuation to complex space of the normal coordinate to the mesh termination. The resultant fields in the complex space do not obey Maxwell's equations. However, it is demonstrated that, through simple field transformations, a new set of fields can be introduced so that they obey Maxwell's equations for an anisotropic medium with properly chosen constitutive parameters depending on the local radii of curvature. The formulation presented here recovers, as particular cases, the previously proposed Cartesian, cylindrical, and spherical PMLs. A previously employed anisotropic (quasi-) PML for conformal terminations is shown to be the large radius of curvature approximation of the anisotropic conformal PML derived herein.* © 1998 John Wiley & Sons, Inc. Microwave Opt Technol Lett 17: 231–236, 1998.

Key words: *absorbing boundary condition; absorbing media; electromagnetic scattering*

1. INTRODUCTION

The simulation of open-region scattering problems using a partial differential equation (PDE) solver usually requires absorbing boundary conditions (ABCs) [1] to properly truncate the computational domain and to maintain the sparsity of the resultant matrices. In 1994, a new material ABC, the perfectly matched layer (PML), was introduced in the literature [2, 3], and since then, it has been extensively studied [4–14]. Being a material ABC, the PML leads naturally to sparse systems, is well suited for parallel implementation, and, consequently, very attractive for computational purposes.

The original PML concept applied only to Cartesian coordinates (planar interfaces). To extend its range of applicability, the PML concept was later extended to nonorthogonal FDTD grids with good results [13, 14]. However, an approximate impedance matching condition was used since the perfect matching condition was derived based on the assumption of the metric coefficients to be independent of the spatial coordinates.

More recently, true PMLs, in the sense of providing reflectionless absorption in the continuum limit, were derived for 2-D cylindrical [15–19], 3-D cylindrical [20], and 3-D spherical interfaces [17, 18, 20].

As with any ABC, it is of interest to investigate the possibility to further extend the PML concept to a conformal PML. Along with its natural flexibility, a conformal ABC has the advantage of promoting, when used in combination with conformal computational grids, a further reduction in the amount of buffer space in the computational domain around the scatterer.

A previous attempt [21] to derive a conformal PML was only partially successful in the sense that a true PML was not obtained, but only an approximate one. This approximate PML (quasi-PML) gives a perfect matching condition only in the limit when the local radii of curvature go to infinity (then it recovers the Cartesian PML). However, even with this approximation, quite encouraging results were obtained in finite-element (FEM) simulations [21].

In this work, we present an analytic derivation of the true 3-D conformal PML on a general orthogonal curvilinear coordinate system. It is demonstrated that the conformal PML can be expressed in terms of an anisotropic constitutive tensor depending on the local principal radii of curvatures of the termination surface. The derivation is based on the complex coordinate stretching approach [5, 6] through a complex stretching (analytic continuation to the upper half plane) of the normal coordinate along the PML (or termina-

tion surface). The previously derived PMLs in Cartesian, cylindrical, and spherical coordinates are shown to be special cases of this conformal PML. The quasi-PML is shown to be the zeroth-order approximation of the anisotropic conformal PML for large radii of curvature.

Throughout this work, the convention $e^{-i\omega t}$ is adopted.

2. CONFORMAL PERFECTLY MATCHED LAYER

We start by introducing a convex (when viewed from the outside), closed surface S around the scatterer(s), representing the interface between free space and the PML region, as illustrated in Figure 1. For a concave scatterer or for a group of scatterers, such a surface can always be chosen given by considering its convex hull. Note that a convex surface S defines a concave surface PML as seen from inside the computational domain. The restriction to a concave PML is an important one, as will be discussed later.

At any given point P on S, a local, right-handed reference frame can be defined through the orthonormal vectors $\mathbf{u}_1$, $\mathbf{u}_2$, $\mathbf{u}_3$. The unit vectors $\mathbf{u}_1$ and $\mathbf{u}_2$ are tangent to S at P along the principal lines of curvature, and $\mathbf{u}_3 = \mathbf{u}_1 \times \mathbf{u}_2$ is the unit vector that is outwardly normal to S at this point. In terms of local coordinates ξ_1, ξ_2, ξ_3, we write $\mathbf{u}_i = (\partial \mathbf{r}/\partial \xi_i)/|\partial \mathbf{r}/\partial \xi_i|$, $i = 1, 2, 3$, where $\mathbf{r}$ is the position vector. This reference frame is called a Darboux frame, and the first fundamental form induced by the coordinates ξ_1 and ξ_2 on the surface S is diagonal [22]. As a consequence, the curvilinear coordinate system ξ_1, ξ_2, ξ_3 is orthogonal having a diagonal metric. Any point P' in this local reference frame is uniquely denoted by the local coordinates ξ_1, ξ_2, ξ_3. The equation $\xi_3 = 0$ represents the surface S. The points of constant ξ_3 corresponds to parallel surfaces in distance ξ_3 to S, and the unit vectors are functions of ξ_1 and ξ_2, only: $\mathbf{u}_1 = \mathbf{u}_1(\xi_1, \xi_2)$, $\mathbf{u}_2 = \mathbf{u}_2(\xi_1, \xi_2)$, $\mathbf{u}_3 = \mathbf{u}_3(\xi_1, \xi_2)$. If the principal radii of curvature at the point P in S are given by $r_{01}(\xi_1, \xi_2)$ and $r_{02}(\xi_1, \xi_2)$ (both positive for S convex), then at a point P', they will be given by $r_1(\xi_1, \xi_2, \xi_3) = r_{01}(\xi_1, \xi_2) + \xi_3$ and $r_2(\xi_1, \xi_2, \xi_3) = r_{02}(\xi_1, \xi_2) + \xi_3$.

It is well known that in any orthogonal system of curvilinear coordinates ξ_1, ξ_2, ξ_3 defined by the diagonal metric $g_{ij} = g_{ii}\delta_{ij}$ with $g_{ii} = h_i^2$, $i = 1, 2, 3$, the Maxwell's equations for an isotropic medium are written as [23]

$$\frac{1}{h_2 h_3}\left[\frac{\partial}{\partial \xi_2}(h_3 E_3) - \frac{\partial}{\partial \xi_3}(h_2 E_2)\right] - i\omega\mu H_1 = 0 \quad (1a)$$

$$\frac{1}{h_3 h_1}\left[\frac{\partial}{\partial \xi_3}(h_1 E_1) - \frac{\partial}{\partial \xi_1}(h_3 E_3)\right] - i\omega\mu H_2 = 0 \quad (1b)$$

$$\frac{1}{h_1 h_2}\left[\frac{\partial}{\partial \xi_1}(h_2 E_2) - \frac{\partial}{\partial \xi_2}(h_1 E_1)\right] - i\omega\mu H_3 = 0 \quad (1c)$$

$$\frac{\partial}{\partial \xi_1}(h_2 h_3 \epsilon E_1) + \frac{\partial}{\partial \xi_2}(h_3 h_1 \epsilon E_2) + \frac{\partial}{\partial \xi_3}(h_1 h_2 \epsilon E_3) = h_1 h_2 h_3 \rho \quad (2)$$

$$\frac{1}{h_2 h_3}\left[\frac{\partial}{\partial \xi_2}(h_3 H_3) - \frac{\partial}{\partial \xi_3}(h_2 H_2)\right] + i\omega\epsilon E_1 = J_1 \quad (3a)$$

$$\frac{1}{h_3 h_1}\left[\frac{\partial}{\partial \xi_3}(h_1 H_1) - \frac{\partial}{\partial \xi_1}(h_3 H_3)\right] + i\omega\epsilon E_2 = J_2 \quad (3b)$$

$$\frac{1}{h_1 h_2}\left[\frac{\partial}{\partial \xi_1}(h_2 H_2) - \frac{\partial}{\partial \xi_2}(h_1 H_1)\right] + i\omega\epsilon E_3 = J_3 \quad (3c)$$

$$\frac{\partial}{\partial \xi_1}(h_2 h_3 \mu H_1) + \frac{\partial}{\partial \xi_2}(h_3 h_1 \mu H_2) + \frac{\partial}{\partial \xi_3}(h_1 h_2 \mu H_3) = 0. \quad (4)$$

Using the local coordinate system defined above, we have $h_1 = r_1/r_{01}$, $h_2 = r_2/r_{02}$, and $h_3 = 1$.

It has been previously observed [17–20] that the modified Maxwell's equations for PML media in Cartesian, cylindrical, and spherical coordinates reduce to the ordinary Maxwell's equations on a complex space, where the x, y, z (Cartesian), ρ, z (cylindrical), and r (spherical) coordinates are analytically continued to a complex space to achieve a reflectionless absorption on the corresponding directions.

In strict analogy to the Cartesian, cylindrical, and spherical PMLs, the conformal PML can be obtained through a complex stretching (analytic continuation to the upper-half complex plane) on the normal coordinate ξ_3:

$$\xi_3 \to \tilde{\xi}_3 = \int_0^{\xi_3} s(\zeta)\, d\zeta = \int_0^{\xi_3}\left(a(\zeta) + i\frac{\sigma(\zeta)}{\omega}\right) d\zeta = b(\xi_3) + i\frac{\Delta(\xi_3)}{\omega} \quad (5)$$

where $a \geq 1$ and $\sigma \geq 0$

The effect of this stretching on a vector propagating wave can be seen, e.g., by locally expanding the wave in terms of a generalized Wilcox expansion [24, 25] in terms of the coordinates ξ_1, ξ_2, ξ_3:

$$\mathbf{E}(\xi_1, \xi_2, \xi_3) = \frac{e^{ik_0\xi_3}}{4\pi(r_1 r_2)^{1/2}} \sum_{n=0}^{+\infty} \frac{\mathbf{E}_n(\xi_1, \xi_2)}{(r_1 r_2)^{n/2}} \quad (6)$$

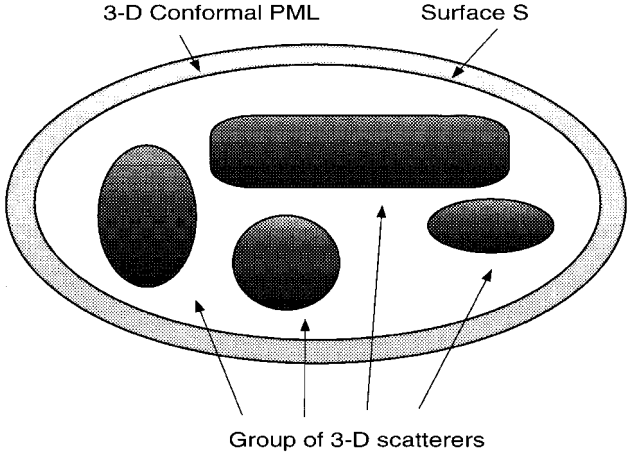

Figure 1

where $k_0 = \omega/c$. Note that (as observed in [24]) the lowest order term in (6) corresponds to the geometrical optics spreading factor for a doubly curved wavefront. By applying the mapping (5) in (6), we arrive at

$$\mathbf{E}(\xi_1, \xi_2, \tilde{\xi}_3) = \frac{e^{-c^{-1}\Delta(\xi_3)} e^{ik_0 b(\xi_3)}}{4\pi(\tilde{r}_1\tilde{r}_2)^{1/2}} \sum_{n=0}^{+\infty} \frac{\mathbf{E}_n(\xi_1, \xi_2)}{(\tilde{r}_1\tilde{r}_2)^{n/2}} \quad (7)$$

where $\tilde{r}_1 = r_{01} + \tilde{\xi}_3$, $\tilde{r}_2 = r_{02} + \tilde{\xi}_3$, and the induced exponential decay along the normal coordinate for $\sigma \geq 0$ is evident. Also, if $a \geq 1$, additional attenuation can be achieved for evanescent waves, if they exist. This is in analogy to the Cartesian PML. Note also that the complex stretching on the normal coordinate preserves the transverse boundary conditions over the PML interface. However, the field in (7) does not obey Maxwell's equations: instead, the substitution of (5) in (1)–(4) leads to the following set of equations inside the conformal PML:

$$\frac{1}{\tilde{h}_2}\left[\frac{\partial}{\partial\xi_2}(E_3) - \frac{1}{s}\frac{\partial}{\partial\xi_3}(\tilde{h}_2 E_2)\right] - i\omega\mu H_1 = 0 \quad (8a)$$

$$\frac{1}{\tilde{h}_1}\left[\frac{1}{s}\frac{\partial}{\partial\xi_3}(\tilde{h}_1 E_1) - \frac{\partial}{\partial\xi_1}(E_3)\right] - i\omega\mu H_2 = 0 \quad (8b)$$

$$\frac{1}{\tilde{h}_1\tilde{h}_2}\left[\frac{\partial}{\partial\xi_1}(\tilde{h}_2 E_2) - \frac{\partial}{\partial\xi_2}(\tilde{h}_1 E_1)\right] - i\omega\mu H_3 = 0 \quad (8c)$$

$$\frac{\partial}{\partial\xi_1}(\tilde{h}_2\epsilon E_1) + \frac{\partial}{\partial\xi_2}(\tilde{h}_1\epsilon E_2) + \frac{1}{s}\frac{\partial}{\partial\xi_3}\left(\tilde{h}_1\tilde{h}_2\epsilon E_3\right) = 0 \quad (9)$$

$$\frac{1}{\tilde{h}_2}\left[\frac{\partial}{\partial\xi_2}(H_3) - \frac{1}{s}\frac{\partial}{\partial\xi_3}(\tilde{h}_2 H_2)\right] + i\omega\epsilon E_1 = 0 \quad (10a)$$

$$\frac{1}{\tilde{h}_1}\left[\frac{1}{s}\frac{\partial}{\partial\xi_3}(\tilde{h}_1 H_1) - \frac{\partial}{\partial\xi_1}(H_3)\right] + i\omega\epsilon E_2 = 0 \quad (10b)$$

$$\frac{1}{\tilde{h}_1\tilde{h}_2}\left[\frac{\partial}{\partial\xi_1}(\tilde{h}_2 H_2) - \frac{\partial}{\partial\xi_2}(\tilde{h}_1 H_1)\right] + i\omega\epsilon E_3 = 0 \quad (10c)$$

$$\frac{\partial}{\partial\xi_1}(\tilde{h}_2\mu H_1) + \frac{\partial}{\partial\xi_2}(\tilde{h}_1\mu H_2) + \frac{1}{s}\frac{\partial}{\partial\xi_3}\left(\tilde{h}_1\tilde{h}_2\mu H_3\right) = 0 \quad (11)$$

where we used $\tilde{h}_1 = \tilde{r}_1/r_{01}$, $\tilde{h}_2 = \tilde{r}_2/r_{02}$ (since these metric coefficients are functions of ξ_3 and must be changed accordingly), $h_3 = 1$, and $\partial/\partial\tilde{\xi}_3 = (1/s)(\partial/\partial\xi_3)$. No sources are assumed inside the PML.

A system of differential equations first order in time can be derived from (8) and (10) with the aid of auxiliary fields, in a manner very similar to [18]. A time-stepping scheme can then be easily implemented. The most salient feature of (8)–(11) (in addition to its complicated appearance!) is that the fields E_i, H_i inside the PML do not satisfy the original Maxwell's equations.

We can summarize some basic properties of this new system of partial differential equations, in the case of a concave PML, as follows.

1. In the physical region (i.e., where $s = 1$), it reduces to the usual Maxwell's equations.
2. Any closed-form field solution of the Maxwell's equations in this general orthogonal curvilinear system can be mapped to solutions of this new system through a simple analytic continuation on the normal variable: $\xi_3 \to \tilde{\xi}_3$, as done in the passage from Eq. (6) to Eq. (7). No reflected field is induced due to this analytic continuation (in the continuum).
3. This analytic continuation preserves the analyticity of the solutions on the upper-half complex ω-plane, as long as we limit ourselves to positive radii of curvature ($r_{01} > 0$ and $r_{02} > 0$) (concave or planar PML). This means that, in this case, the resultant frequency-domain solutions are still causal in terms of a real-axis Fourier inversion contour or, equivalently, that the solutions are dynamically stable. Otherwise (nonconcave, nonplanar PML), the solutions will contain singularities in the upper-half plane, implying time-domain solutions that may grow unbounded. This will be discussed in more detail later.

The fact that this system of equations is not the original Maxwell's equations is a drawback for some applications. In the next section, we show how to build a conformal PML formulation from (8)–(11) which satisfies Maxwell's equations with an anisotropic medium.

3. ANISOTROPIC CONFORMAL PERFECTLY MATCHED ABSORBER

In this section, we describe how to develop a conformal anisotropic PML absorber for the Maxwell's equations from the previous complex-space formulation. This is particularly useful for applying the conformal PML to methods such as the FEM.

We start by introducing a new set of fields $\tilde{E}_i$, $\tilde{H}_i$ obtained by using the following transformations on the E_i, H_i fields of (8)–(11): $\tilde{E}_1 = (\tilde{h}_1/h_1)E_1$, $\tilde{E}_2 = (\tilde{h}_2/h_2)E_2$, $\tilde{E}_3 = sE_3$, $\tilde{H}_1 = (\tilde{h}_1/h_1)H_1$, $\tilde{H}_2 = (\tilde{h}_2/h_2)H_2$, $\tilde{H}_3 = sH_3$.

We note that, since the factors $(\tilde{h}_i/h_i)$ are continuous along the free-space–PML interface (both r_i and $\tilde{\xi}_3$ are continuous), the original tangential fields E_1, H_1, E_2, H_2 and the transformed tangential fields $\tilde{E}_1$, $\tilde{H}_1$, $\tilde{E}_2$, $\tilde{H}_2$ obey the same set of boundary conditions at the free-space–PML interface. Therefore, since E_1, H_1, E_2, H_2 are perfectly matched at this interface, $\tilde{E}_1$, $\tilde{H}_1$, $\tilde{E}_2$, $\tilde{H}_2$ are also perfectly matched.

Furthermore, by substituting the transformed fields into (8)–(11), we arrive at the equations

$$\frac{1}{h_2}\left[\frac{\partial}{\partial\xi_2}\tilde{E}_3 - \frac{\partial}{\partial\xi_3}(h_2\tilde{E}_2)\right] - i\omega\mu\left(\frac{s\tilde{h}_1\tilde{h}_2}{\tilde{h}_1 h_2}\right)\tilde{H}_1 = 0 \quad (12a)$$

$$\frac{1}{h_1}\left[\frac{\partial}{\partial\xi_3}(h_1\tilde{E}_1) - \frac{\partial}{\partial\xi_1}\tilde{E}_3\right] - i\omega\mu\left(\frac{s\tilde{h}_1 h_2}{h_1\tilde{h}_2}\right)\tilde{H}_2 = 0 \quad (12b)$$

$$\frac{1}{h_1 h_2}\left[\frac{\partial}{\partial\xi_1}(h_2\tilde{E}_2) - \frac{\partial}{\partial\xi_2}(h_1\tilde{E}_1)\right] - i\omega\mu\left(\frac{\tilde{h}_1\tilde{h}_2}{sh_1 h_2}\right)\tilde{H}_3 = 0 \quad (12c)$$

$$\frac{\partial}{\partial \xi_1}\left[h_2\epsilon\left(\frac{sh_1\tilde{h}_2}{\tilde{h}_1h_2}\right)\tilde{E}_1\right]+\frac{\partial}{\partial \xi_2}\left[h_1\epsilon\left(\frac{s\tilde{h}_1h_2}{h_1\tilde{h}_2}\right)\tilde{E}_2\right]+\frac{\partial}{\partial \xi_3}\left[h_1h_2\epsilon\left(\frac{\tilde{h}_1\tilde{h}_2}{sh_1h_2}\right)\tilde{E}_3\right]=0 \quad (13)$$

$$\frac{1}{h_2}\left[\frac{\partial}{\partial \xi_2}\tilde{H}_3-\frac{\partial}{\partial \xi_3}(h_2\tilde{H}_2)\right]+i\omega\epsilon\left(\frac{sh_1\tilde{h}_2}{\tilde{h}_1h_2}\right)\tilde{E}_1=0 \quad (14a)$$

$$\frac{1}{h_1}\left[\frac{\partial}{\partial \xi_3}(h_1\tilde{H}_1)-\frac{\partial}{\partial \xi_1}\tilde{H}_3\right]+i\omega\epsilon\left(\frac{s\tilde{h}_1h_2}{h_1\tilde{h}_2}\right)\tilde{E}_2=0 \quad (14b)$$

$$\frac{1}{h_1h_2}\left[\frac{\partial}{\partial \xi_1}(h_2\tilde{H}_2)-\frac{\partial}{\partial \xi_2}(h_1\tilde{H}_1)\right]+i\omega\epsilon\left(\frac{\tilde{h}_1\tilde{h}_2}{sh_1h_2}\right)\tilde{E}_3=0 \quad (14c)$$

$$\frac{\partial}{\partial \xi_1}\left[h_2\mu\left(\frac{sh_1\tilde{h}_2}{\tilde{h}_1h_2}\right)\tilde{H}_1\right]+\frac{\partial}{\partial \xi_2}\left[h_1\mu\left(\frac{s\tilde{h}_1h_2}{h_1\tilde{h}_2}\right)\tilde{H}_2\right]+\frac{\partial}{\partial \xi_3}\left[h_1h_2\mu\left(\frac{\tilde{h}_1\tilde{h}_2}{sh_1h_2}\right)\tilde{H}_3\right]=0. \quad (15)$$

A careful look at Eqs. (12)–(15) reveals that they are just the Maxwell's equations on the original orthogonal curvilinear coordinates system of (1)–(4) characterized by the (real) metric $g_{ij}=g_{ii}\delta_{ij}$ with $g_{ii}=h_i^2$, $i=1,2,3$, and $h_3=1$, but now for an anisotropic medium, whose constitutive parameters are given by $\bar{\bar{\mu}}=\mu\bar{\bar{\Lambda}}$ and $\bar{\bar{\epsilon}}=\epsilon\bar{\bar{\Lambda}}$, with

$$\bar{\bar{\Lambda}}=\mathbf{u}_1\mathbf{u}_1\left(\frac{sh_1\tilde{h}_2}{\tilde{h}_1h_2}\right)+\mathbf{u}_2\mathbf{u}_2\left(\frac{s\tilde{h}_1h_2}{h_1\tilde{h}_2}\right)+\mathbf{u}_3\mathbf{u}_3\left(\frac{\tilde{h}_1\tilde{h}_2}{sh_1h_2}\right). \quad (16)$$

The significance of this result is that it is possible to achieve reflectionless absorption of electromagnetic waves incident on a smooth, concave surface having anisotropic constitutive tensors given by (16), depending on the local principal radii of curvatures. Note that since (16) is a formula of a constitutive parameter, it is independent of any coordinate system. This simply means that, given a concave surface termination (as viewed from inside), we can apply this anisotropic conformal PML in any coordinate system by expressing the local radii of curvature and the stretching as functions of the new coordinates, so that $\bar{\bar{\Lambda}}=\bar{\bar{\Lambda}}(\mathbf{r})$ is a function of $\mathbf{r}$ only.

An interesting point to observe is the local interplay between the physics of the medium and the geometry, as the (local) constitutive parameters depend on the (local) geometry of the termination.

Note also that the computational realization of such an absorber in the FEM does not pose a great challenge and can be done, e.g., via an isoparametric mapping [21].

4. SOME SPECIAL CASES

4.1. Cartesian Case. The previously derived Cartesian [7], cylindrical [15, 20], and spherical [20] anisotropic PML are just special cases of (16). The Cartesian PML is obtained by setting $r_{01}=r_{02}=\infty$, so that $\tilde{h}_1=\tilde{h}_2=1$. Furthermore, if $\mathbf{u}_1=\mathbf{u}_x$, $\mathbf{u}_2=\mathbf{u}_y$, $\mathbf{u}_3=\mathbf{u}_z$, and $s=s_z(z)$ for attenuation in the z-direction, then (16) becomes

$$\bar{\bar{\Lambda}}_z(z)=\mathbf{u}_x\mathbf{u}_xs_z+\mathbf{u}_y\mathbf{u}_ys_z+\mathbf{u}_z\mathbf{u}_z\frac{1}{s_z}, \quad (17)$$

as first derived in [7]. Since $\bar{\bar{\Lambda}}_z(z)$ is a function of z only, we can combine it with simultaneous stretching in the x- and y-directions (orthogonal everywhere) also:

$$\bar{\bar{\Lambda}}_{x,y,z}(x,y,z)=\bar{\bar{\Lambda}}_x(x)\cdot\bar{\bar{\Lambda}}_y(y)\cdot\bar{\bar{\Lambda}}_z(z)=\mathbf{u}_x\mathbf{u}_x\frac{s_ys_z}{s_x}+\mathbf{u}_y\mathbf{u}_y\frac{s_zs_x}{s_y}+\mathbf{u}_z\mathbf{u}_z\frac{s_xs_y}{s_z}, \quad (18)$$

which is the most general expression for the Cartesian PML and corresponds to a corner region.

4.2. Cylindrical Case. The cylindrical PML is obtained by setting $r_{01}=\infty$, $r_{02}=\rho$, so that $\tilde{h}_1=1$ and $\tilde{h}_2=\tilde{\rho}/\rho$. Furthermore, $\mathbf{u}_1=\mathbf{u}_\phi$, $\mathbf{u}_2=\mathbf{u}_z$, $\mathbf{u}_3=\mathbf{u}_\rho$, and $s=s_\rho(\rho)$ for attenuation in the ρ-direction, so that (16) becomes

$$\bar{\bar{\Lambda}}_{\rho,\phi}(\rho)=\mathbf{u}_\phi\mathbf{u}_\phi\frac{\rho s_\rho}{\tilde{\rho}}+\mathbf{u}_z\mathbf{u}_z\frac{\tilde{\rho}s_\rho}{\rho}+\mathbf{u}_\rho\mathbf{u}_\rho\frac{\tilde{\rho}}{\rho s_\rho}, \quad (19)$$

as first derived using a graphical method in [15].

Since $\bar{\bar{\Lambda}}_\rho(\rho)$ is a function of ρ only, we can combine it with a simultaneous stretching (Cartesian) on the z-direction (orthogonal to ρ everywhere) also:

$$\bar{\bar{\Lambda}}_{\rho,\phi,z}(\rho,z)=\bar{\bar{\Lambda}}_\rho(\rho)\cdot\bar{\bar{\Lambda}}_z(z)=\mathbf{u}_\phi\mathbf{u}_\phi\frac{\rho s_zs_\rho}{\tilde{\rho}}+\mathbf{u}_z\mathbf{u}_z\frac{\tilde{\rho}s_\rho}{\rho s_z}+\mathbf{u}_\rho\mathbf{u}_\rho\frac{\tilde{\rho}s_z}{\rho s_\rho}, \quad (20)$$

which is the most general expression for the 3-D cylindrical PML, as derived in [20].

4.3. Spherical Case. The spherical PML is obtained by setting $r_{01}=r_{02}=r$, so that $\tilde{h}_1=\tilde{h}_2=\tilde{r}/r$. Furthermore, $\mathbf{u}_1=\mathbf{u}_\theta$, $\mathbf{u}_2=\mathbf{u}_\phi$, $\mathbf{u}_3=\mathbf{u}_r$, and $s=s_r(r)$ for attenuation in the r-direction, so that (16) becomes

$$\bar{\bar{\Lambda}}_{r,\phi,\theta}(r)=\mathbf{u}_r\mathbf{u}_r\left(\frac{\tilde{r}}{r}\right)^2\frac{1}{s_r}+\mathbf{u}_\phi\mathbf{u}_\phi s_r+\mathbf{u}_\theta\mathbf{u}_\theta s_r, \quad (21)$$

as derived in [20].

4.4. Large Radius of Curvature Approximation. If $r_{01}, r_{02}\gg\lambda$, then we have, as a zeroth-order approximation for (16):

$$\bar{\bar{\Lambda}}=\mathbf{u}_1\mathbf{u}_1s+\mathbf{u}_2\mathbf{u}_2s+\mathbf{u}_3\mathbf{u}_3\frac{1}{s}, \quad (22)$$

which is just the planar PML with stretching in the normal direction, as considered in [21]. This approximation should be more properly called "quasi-PML" [26]. As demonstrated in [21], very good results can be obtained with this approximation, as long as large radius of curvature is considered, which is the case for large scatterers.

Care must be taken to derive higher order approximations to (16). For instance, it is easy to show that the first-order approximation using a Taylor expansion in λ/r_{01}, λ/r_{02} to (16) gives rise to constitutive tensors having poles on the upper-half ω-plane for any $r_{01}\neq r_{02}$. This implies an active-

medium behavior, and the resultant time-domain equations may turn out to by dynamically unstable, as discussed in the next section.

5. CAUSALITY AND STABILITY ISSUES FOR THE CONFORMAL PML

As discussed in more detail elsewhere [27], a condition that should be investigated for the frequency-dependent matrix $\overline{\overline{\Lambda}}$ (and also its inverse $\overline{\overline{\Lambda}}^{-1}$) is whether it violates causality in the sense of the real axis Fourier inversion contour. This is equivalent to having the upper-half complex ω-plane free of singularities (and zeros).

Using the stretching defined by (5), it can be easily shown that, for a concave or planar surface PML (more precisely, $r_{01} > 0$ and $r_{02} > 0$), all poles and zeros of $\overline{\overline{\Lambda}}$ are on the lower-half plane, so that causality is not violated. However, for a nonconcave, nonplanar surface PML (i.e., $r_{01} < 0$ or $r_{02} < 0$), there will be poles and zeros on the upper-half plane.

In the latter case, causality in the sense of real-axis integration is violated. In time-domain explicit methods, such as the FDTD, the causality will necessarily be enforced, which is equivalent to taking the Fourier inversion contour to be above all singularities [1]. In this case, the PML will behave as an active medium, and the resultant time-domain equations may turn out to be dynamically unstable, as, for instance, was found to be the case for simulations employing cylindrical and spherical convex PMLs (inner boundary) [27]. An alternative to ensure a dynamically stable ABC when $r_{01} < 0$ or $r_{02} < 0$ (although not perfectly matched anymore) is to use the "quasi-PML" described in the previous section.

This violation of causality can also be directly checked by an investigation of the singularities in the resultant analytic solutions, such as (7). For a concave PML, the denominator factors in (7) produce branch points and/or poles only in the lower-half plane (the singularities present on (6) are translated downward in the complex ω-plane). For a noncave, nonplanar PML, however, these singularities are present on the upper-half plane (the singularities present on (6) are translated upward in the ω complex plane).

It is important to note that these conclusions are valid by considering the stretching defined by (5), which is universally used in the literature. For other kinds of stretching (which would imply more involved time-domain equations), they are not necessarily valid.

6. CONCLUSIONS

An analytic derivation of a conformal PML for concave grid terminations is presented. The derivation is based on the complex stretching of the normal direction on a generalized orthogonal curvilinear coordinate system conformal to a termination surface.

It is shown that this conformal PML produces an exponential decay of the fields in the normal direction without any reflections in the continuum limit. In the complex-space formulation, the resultant fields do not obey Maxwell's equations. However, an alternative formulation is presented with anisotropic medium where the fields obey the Maxwell's equations everywhere. In analogy with the Cartesian, cylindrical, and spherical PMLs, in this Maxwellian formulation, the PML region is represented by an anisotropic artificial medium. For the conformal PML, the constitutive tensors depend on the local radii of curvature of the termination surface.

ACKNOWLEDGMENTS

This work was supported by the AFOSR under MURI Grant F49620-96-1-0025, the ONR under Grant N00014-95-1-0872, the NSF under Grant ECS93-02145, and a CAPES Fellowship.

REFERENCES

1. W. C. Chew, *Waves and Fields in Inhomogeneous Media*, Van Nostrand, New York, 1990, Chap. 4 (reprinted by IEEE Press, 1995).
2. J. Berenger, "A Perfectly Matched Layer for the Absorption of Electromagnetic Waves," *J. Comput. Phys.*, Vol. 114, No. 2, 1994, pp. 185–200.
3. J. Berenger, "Three-Dimensional Perfectly Matched Layer for the Absorption of Electromagnetic Waves," *J. Comput. Phys.*, Vol. 127, No. 2, 1996, pp. 363–379.
4. D. S. Katz, T. Thiele, and A. Taflove, "Validation and Extension to Three Dimensions of the Berenger PML Absorbing Boundary Condition," *IEEE Microwave Guided Wave Lett.*, Vol. 4, No. 8, 1994, pp. 268–270.
5. W. C. Chew and W. Weedon, "A 3D Perfectly Matched Medium from Modified Maxwell's Equations with Stretched Coordinates," *Microwave Opt. Technol. Lett.*, Vol. 7, No. 13, 1994, pp. 599–604.
6. C. M. Rappaport, "Interpreting and Improving the PML Absorbing Boundary Condition Using Anisotropic Lossy Mapping of Space," *IEEE Trans. Magn.*, Vol. 32, No. 3, 1996, pp. 968–974.
7. Z. S. Sacks, D. M. Kingsland, R. Lee, and J.-F. Lee, "A Perfectly Matched Anisotropic Absorber for Use as an Absorbing Boundary Condition," *IEEE Trans. Antennas Propagat.*, Vol. 43, Dec. 1995, pp. 1460–1463.
8. S. D. Gedney, "An Anisotropic PML Absorbing Media for the FDTD Simulation of Fields in Lossy and Dispersive Media," *Electromagn.*, Vol. 16, 1996, pp. 399–415.
9. L. Zhao and A. C. Cangellaris, "GT-PML: Generalized Theory of Perfectly Matched Layers and Its Application to the Reflectionless Truncation of Finite-Difference Time-Domain Grids," *IEEE Trans. Microwave Theory Tech.*, Vol. 44, Dec. 1996, pp. 2555–2563.
10. W. C. Chew and J. M. Jin, "Perfectly Matched Layers in the Dicretized Space: An Analysis and Optimization," *Electromagn.*, Vol. 16, 1996, pp. 325–340.
11. N. Kantartzis and T. Tsiboukis, "A Comparative Study of the Berenger Perfectly Matched Layer, the Superabsorption Technique and Several High-Order ABC's for the FDTD Algorithm in Two and Three Dimensional Problems," *IEEE Trans. Magn.*, Vol. 33, No. 2, 1996, pp. 1460–1463.
12. J.-Y. Wu, D. M. Kingsland, J.-F. Lee, and R. Lee, "A Comparison of Anisotropic PML to Berenger's PML and Its Application to the Finite-Element Method for EM Scattering," *IEEE Trans. Antennas Propagat.*, Vol. 45, Jan. 1997, pp. 40–50.
13. E. A. Navarro, C. Wu, P. Y. Chung, and J. Litva, "Application of PML Superabsorbing Boundary Condition to Non-Orthogonal FDTD Method," *Electron. Lett.*, Vol. 30, No. 20, 1994, pp. 1654–1655.
14. J. A. Roden and S. D. Gedney, "Efficient Implementation of the Uniaxial-Based PML Media in Three-Dimensional Nonorthogonal Coordinates with the Use of the FDTD Technique," *Microwave Opt. Technol. Lett.*, Vol. 14, No. 2, 1997, pp. 71–75.
15. J. Maloney, M. Kesler, and G. Smith, "Generalization of PML to Cylindrical Geometries," *Proc. 13th Annu. Rev. Prog. Appl. Comp. Electromagn.*, Vol. 2, Monterey, CA, Mar. 1997, pp. 900–908.
16. B. Yang, D. Gottlieb, and J. S. Hesthaven, "On the Use of PML ABC's in Spectral Time-Domain Simulations of Electromagnetic Scattering," *Proc. 13th Annu. Rev. Prog. Appl. Comp. Electromagn.*, Vol. 2, Monterey, CA, Mar. 1997, pp. 926–933; see also B. Yang, D. Gottlieb, and J. S. Hesthaven, "Spectral Simulations of Electromagnetic Wave Scattering," *J. Comput. Phys.*, Vol. 134, 1997, pp. 216–230.

17. W. C. Chew, J. M. Jin, and E. Michielssen, "Complex Coordinate System as a Generalized Absorbing Boundary Condition," *Proc. 13th Annu. Rev. Prog. Appl. Comp. Electromagn.*, Vol. 2, Monterey, CA, Mar. 1997, pp. 909–914; see also W. C. Chew, J. M. Jin, and E. Michielssen, "Complex Coordinate Stretching as a Generalized Absorbing Boundary Condition," *Microwave Opt. Technol. Lett.*, Vol. 15, No. 6, 1997, pp. 363–369.
18. F. L. Teixeira and W. C. Chew, "PML-FDTD in Cylindrical and Spherical Grids," *IEEE Microwave Guided Wave Lett.*, Vol. 7, No. 9, 1997, pp. 285–287.
19. F. Collino and P. Monk, "The Perfectly Matched Layer in Curvilinear Coordinates," private communication.
20. F. L. Teixeira and W. C. Chew, "Systematic Derivation of Anisotropic PML Absorbing Media in Cylindrical and Spherical Coordinates," *IEEE Microwave Guided Wave Lett.*, Vol. 7, No. 11, 1997.
21. M. Kuzuoglu and R. Mittra, "Investigation of Nonplanar Perfectly Matched Absorbers for Finite-Element Mesh Truncation," *IEEE Trans. Antennas Propagat.*, Vol. 45, Mar. 1997, pp. 474–486.
22. H. W. Guggenheimer, *Differential Geometry*, Dover, New York, 1977, pp. 206–214.
23. J. A. Stratton, *Electromagnetic Theory*, McGraw-Hill, New York, 1941, pp. 50–51.
24. A. Chatterjee and J. L. Volakis, "Conformal Absorbing Boundary Conditions for the Vector Wave Equation," *Microwave Opt. Technol. Lett.*, Vol. 6, No. 16, 1993, pp. 886–889; "Correction to 'Conformal Absorbing Boundary Conditions for the Vector Wave Equation,'" *Microwave Opt. Techol. Lett.*, Vol. 8, No. 6, 1995, pp. 323–324.
25. C. H. Wilcox, "An Expansion Theorem for Electromagnetic Fields," *Commun. Pure Appl. Math.*, Vol. 9, 1956, pp. 115–1334.
26. J. Q. He and Q. H. Liu, "A Non-Uniform Cylindrical FDTD Algorithm with Liao's and Quasi-PML Absorbing Boundary Conditions," private communication.
27. F. L. Teixeira and W. C. Chew, "A Study on Causality and Dynamical Stability of Perfectly Matched Layers for Time-Domain Applications," Center for Computational Electromagnetics, University of Illinois at Urbana–Champaign, Res. Rep., Sept. 1997.

CCC 0895-2477/98

CHARGE CARRIER EFFECT ON THE MICROWAVE LOSSES OBSERVED ON TRAVELING-WAVE ELECTRODES USED IN ELECTRO-OPTIC MODULATORS

H. R. Khazaei,[1] O. Berolo,[1] R. James,[1] W. J. Wang,[1] P. Maigné,[1] M. Young,[2] K. Ozard,[2] M. Reeves,[2] and F. M. Ghannouchi[3]
[1] Communications Research Centre
Ottawa, Ont. K2H 8S2, Canada
[2] Nortel Technology
Ottawa, Ont. K1Y 4H7, Canada
[3] Ecole Polytechnique of Montreal
Montreal, P.Q. H3C 3A7, Canada

Received 26 August 1997

ABSTRACT: *The free charge carrier effect is used to explain and model microwave losses observed in traveling-wave electrodes used in electro-optic modulators when the coplanar waveguide (CPW) electrodes are fabricated on unintentionally doped heterostructure optical ridge waveguides. Microwave losses were measured between 45 MHz and 40 GHz as a function of doping over a range of* $1 \times 10^8 / cm^3 < N_d < 2 \times 10^{18} / cm^3$ *using both epitaxially grown and ion implanted semi-insulating (SI) GaAs substrates. Results show that there is a critical residual doping limit at* $N_d \approx 1 \times 10^{14} / cm^3$*, above which the microwave loss increases linearly with doping for 6 μm thick epitaxially grown materials.* © 1998 John Wiley & Sons, Inc. Microwave Opt Technol Lett 17: 236–241, 1998.

Key words: *microwave loss; slow-wave electrode; electro-optic modulator*

I. INTRODUCTION

The deployment of OC-48 wavelength-division multiplex networks and OC-192 fiber optic communication links foresees the need to achieve high modulator speeds with lasers and laser arrays in the near future [1]. The present direct laser modulation frequency limit is at ~30 GHz [2]. Although laser dynamic processes are well understood [3], this upper limit on frequency modulation has been attributed to the distributed microwave effects associated with the length of the laser cavity and the dimensions of the current-injecting electrode [4, 5]. The distributed circuit approach is not new, as it has played an important role in the design of EHF MESFETs, HEMTs, and HBTs [6]. An alternate solution to this high-frequency limitation of direct-modulated lasers is to implement external modulation techniques.

External laser modulation using millimeter-wave coplanar structures exploit the electro-optic effect [7] and, due to their distributed nature [8], promise to achieve modulation bandwidths in excess of 100 GHz [9]. This is achieved by the use of traveling-wave electrodes which slow the microwave phase velocity, matching it to the phase velocity of the optical signal propagating in the ridge waveguide.

The bulk of the research investigating the design and the performance of CPW traveling-wave structures has been carried out on semi-insulating (SI) material such as GaAs [10, 11] (and references therein) and more recently on InP [9]. The integration of these designs with ridge optical waveguide heterostructures was successfully carried out and small-signal modulation demonstrated by a small number of researchers [12, 13]. Other workers have met with limited success at low modulation bandwidths [14–16]. 300 MHz bandwidths were achieved in [14] for traveling-wave structures defined on n^+ material. These workers concluded that the thickness of the n^+ layer must be reduced to increase the modulator bandwidth. Modeling of CPW structures on semiconductor substrates in [15] demonstrated that an inhomogeneous doping profile in the optical guiding heterostructure would reduce the microwave losses and increase the bandwidth. The high loss in the response curve of the modulator in [16] was attributed to the electrode design for structures which were fabricated on heterostructured optical guides with carrier concentrations at $N_d = 5 \times 10^{17}/\text{cm}^3$. The common factor which ties together the demonstration of slow-wave modulators in [12, 13] and previous work referred to therein is the fact that the semiconducting heterostructures defining the optical waveguide were unintentionally doped. It is widely understood that unintentional doping can mean a residual carrier concentration N_d between $1 \times 10^{14}/\text{cm}^3$ and $5 \times 10^{16}/\text{cm}^3$, depending on the epitaxial material and growth technique used.

This work reports on the microwave loss measurements of a variety of CPW structures defined on epitaxial and ion-implanted GaAs as a function of substrate doping. The doping range under study is between $1 \times 10^8/\text{cm}^3$ (suggested by the manufacturer) and $2 \times 10^{18}/\text{cm}^3$. The loss measurements can be modeled using the effect of the free-carrier interaction with the RF electric field present in the semicon-